Lattice dynamics and self-diffusion in niobium at elevated temperatures

Lattice dynamics and self-diffusion in niobium at elevated temperatures

F Güthoff†‡, B Hennion§, C Herzig‡, W Petry‖, H R Schober¶ and J Trampenau‖

† Institut Laue–Langevin, BP 156, F-38042 Grenoble, France
‡ Institut für Metallforschung, Universität Münster, D-48149 Münster, Germany
§ Laboratoire Léon Brillouin, CEA-Saclay, F-91191 Gif-sur-Yvette Cédex, France
‖ Physik Department E13, Technische Universität München, D-85748 Garching, Germany
¶ Institut für Festkörperforschung der KFA-Jülich, D-52425 Jülich, Germany

Abstract. The temperature dependence of the phonon dispersion of Nb from room temperature up to 2223 K has been measured by means of inelastic neutron scattering. Over a temperature range of nearly 2000 K the dispersion changes only moderately. Effects due to electron–phonon interaction almost vanish at the highest temperature. Parameterizing the dispersion curves by Born–von Kármán force constants, the phonon density of states $g(\omega)$ at different temperatures was computed. Employing the model of phonon controlled diffusion in BCC metals, the migration barrier H^m and the formation entropy S^f have been calculated. The results agree with those of quenching and electron irradiation experiments.

1. Introduction

It is well known that self-diffusion in BCC metals behaves, compared with that of FCC metals, anomalously. This is mirrored not only in the great variance of the diffusivities themselves which at $T = 1/2T_m$ (T_m = melting temperature) extend over nine orders of magnitude but also in a wide spread of activation enthalpies Q ($Q = H^m + H^f$, the sum of migration and formation enthalpies) as well as in pronounced curvatures in the Arrhenius presentation of $D(T)$ [1]. A convenient approach towards understanding the origin of these effects is the study of their—eventually temperature dependent—phonon dispersions [2, 3]. Two aspects are conspicuous in the lattice dynamics of the BCC metals. With the exception of the group VI metals, all BCC elements show a pronounced dip in the vicinity of the longitudinal L2/3(111) (ω-point) mode. It was shown by Falter *et al* [4], for simple s–p bonded metals, that this softening is inherent to the geometry of the BCC structure. With the help of frozen phonon calculations, Ho *et al* [5] explained the variation of the phonon frequencies at the ω-point in BCC metals by the filling of d states. With increasing d electron density stronger directional bonding arises, which effectively enhances the restoring forces between neighbouring [111] chains. Other characteristics are the comparatively low frequencies of the transverse $T_1[\xi\xi 0]$ branch with $[1\bar{1}0]$ polarization. Both features are connected with the tendency of BCC elements to transform into close-packed structures. The L2/3(111) phonon displaces the lattice towards the hexagonal ω-structure, whereas the $T_1[\xi\xi 0]$ branch displaces the lattice towards close-packed stacking sequences (HCP, FCC,...) [6].

Recently we established a close relation between these low-energy phonons and the high diffusion coefficients of the BCC metals [2, 3]. Low phonon energies mean small restoring

forces, i.e. shallow potentials for the corresponding displacements. Now all low-energy phonons either displace the atoms directly into the [111] nearest-neighbour (NN) direction, or their displacement vectors have a considerable projection in that direction. Assuming that the dominant diffusion mechanism is a jump into NN vacancies, i.e. its direction coincides with the displacement vectors of the low-energy phonons, the latter serves as a kind of fingerprint of low migration barriers. A quantitative elaboration of this idea of phonon controlled diffusion allowed the direct calculation of the migration barrier for NN vacancy diffusion [7].

Critical tests of this model are (i) the reproduction of the pronounced variation of $D(T)$ with increasing s and d electron density and (ii) an explanation of the observed curvatures in the Arrhenius plot of $D(T)$. Indeed the lowest L2/3(111) frequencies and the lowest transverse $T_1[\xi\xi0]$ branches are observed in alkali metals. The frequencies increase with increasing s and d electron filling. For the group VI metals Cr, Mo, and W, the dip at L2/3(111) has almost disappeared and the $T_1[\xi\xi0]$ branch has hardened, i.e. it is stiffer than the $T_2[\xi\xi0]$ branch ([001] polarization). Further, there is a decrease in the frequencies of the phase transition related phonons in the BCC phase of the group IV metals Ti, Zr, and Hf. With decreasing temperature they behave as a kind of dynamical precursor of the martensitic BCC to HCP transition. The opposite occurs in Cr or Mo [8,9]. Here BCC is the stable low-temperature configuration and a softening of the L2/3(111) mode and the $T_1[\xi\xi0]$ branch is observed with increasing temperature. All this is in accordance with the observed diffusion coefficients. Whereas in β-Ti the activation energy Q increases with temperature, it decreases in Cr.

Nb as a representative of the group V metals lies between the above two extreme cases and its diffusivity closely resembles that observed in normal FCC metals. Only a slight curvature is discernible in the Arrhenius presentation of $D(T)$ [10–12]. In this paper, we ask how this is reflected in the temperature dependence of the low-energy phonons in Nb. Earlier various dispersion measurements were done up to 1030 K [13], but no diffusion measurements are available at these low temperatures. We therefore measured the lattice dynamics of Nb at 293 K, 773 K, 1773 K, and 2223 K.

Much interest in Nb is concerned with its superconductivity with the relatively high transition temperature of 9.1 K. The influence of Fermi surfaces on the phonon dispersion—such as resonance screening—has been widely investigated (see e.g. [14], [15] and references therein). Even up to very high temperatures, the phonons are affected by this screening. As the formation enthalpy H^f is dominated by electronic effects [16], the question arises of whether this term in the activation enthalpy is also temperature dependent.

2. Experimental details

Two Nb samples (4N purity, cylinders with 6 mm diameter and 50 mm long) with (110) and (100) orientation were prepared by Metal Crystals and Oxides Ltd, Cambridge, UK. The samples were fixed in between pure Nb clamps screwed into the sample support of a furnace. To avoid contamination the vacuum was of the order of 10^{-4} Pa. The temperature was either controlled by W 5%Re/W 26%Re thermocouples or by a calibrated two-colour pyrometer. The temperature was held stable (±2 K) with a temperature gradient at 2223 K of ~ 30 K along the sample axis. For the melting temperature of Nb a value $T_m = 2741$ K has been taken. Different three-axes instruments were used (IN3 at ILL and DN1 at CEN Grenoble, 1T at CEN Saclay, and HB1 at ECN Petten). Most of the inelastic scans were performed at constant scattering vector Q with fixed $k_{f/i} = 2.662$ Å^{-1} and $\lambda/2$ was suppressed by a graphite filter. Typical horizontal collimations were 30' 30' 40' 40' yielding a resolution of

vanadium scans of the order of 0.8 meV FWHM. Several scans were taken twice to check for possible alignment errors at the different instruments.

3. Results

The measurements at room temperature agree well with the results of Powell *et al* [13]. Also at higher temperatures their changes in the dispersion are reproduced—see figure 1. The dispersion curves resemble, in general, those of the other BCC transition metals. Besides a common decrease of phonon frequencies to higher temperatures, some peculiarities are interesting to mention (see figure 2).

(i) For small ξ the $T_2[\xi\xi 0]$ branch with [001] polarization lies below the $T_1[\xi\xi 0]$ branch. They cross at $\xi \simeq 0.20$ RLU. At higher temperatures, the initial slopes of the two branches approach each other. The longitudinal $L[\xi\xi 0]$ branch does not change with temperature within the error bars.

(ii) As pointed out already by Nakagawa and Woods [17] the $T[\xi 00]$ branch first falls below the value of the elastic constant line at $\xi \simeq 0.2$ and then curves upward with increasing ξ. The transverse and the longitudinal branches cross at $\xi \simeq 0.7$ at low temperatures. This cross-over and also the dip at $\xi \simeq 0.7$ of the $L[\xi 00]$ branch vanish at high temperatures. These features can be deduced from the electron–phonon interaction and were discussed in detail in connection with Kohn anomalies [18]. By model calculations Varma and Weber [15] explain these anomalies as a consequence of the highly anisotropic Fermi surfaces.

(iii) Especially the temperature dependence of the L2/3[111] phonon mode differs from other modes, as there is with increasing temperature first an increase in frequency and later a decrease. Also the position of the dip changes and does not coincide with the commensurate value $\xi = \frac{2}{3}$ in the [111] direction.

In first order, the temperature dependences of the phonons in Nb at symmetry points follow a linear law $\partial\omega/\partial T \simeq -1.4 \times 10^{-3}$ meV K^{-1} for the H point phonon, $\simeq -1.7 \times 10^{-3}$ meV K^{-1} for the $T_1 0.5[110]$ phonon and $\simeq -1.5 \times 10^{-3}$ meV K^{-1} for the $T_2 0.5[110]$ phonon. The dispersion curves of Nb and Ta look quite similar but differ from those of the neighbouring group IV and VI elements.

4. Discussion

To have a unified procedure for comparison the dispersion curves at all measured temperatures were analysed with Born–von Kármán tensor forces up to six neighbour shells. The fits of the force constants were constrained to be consistent with the elastic constants measured by ultrasound propagation [19]—see table 1. The resulting force constants are listed in table 2. At room temperature even with longer-range interactions the fit cannot reproduce exactly all the anomalies mentioned before. At 2223 K good fits were achieved even with five neighbour shells. Empirical interaction potentials such as a Finnis–Sinclair potential [20] or a temperature dependent damped pair potential [21] grossly misrepresent the dispersion curves. A better understanding of the electron–phonon interaction and a reasonable reproduction of the phonon dispersion, also in other transition metals and compounds, was achieved by the earlier calculation of Varma and Weber [15]. In their model they rearranged the dynamical matrix in terms of long- and short-range interactions. They showed in their calculations that the phonon anomalies originate from long-range oscillatory force fields, which arise from scattering states near E_F ($\simeq \pm 0.5$ eV).
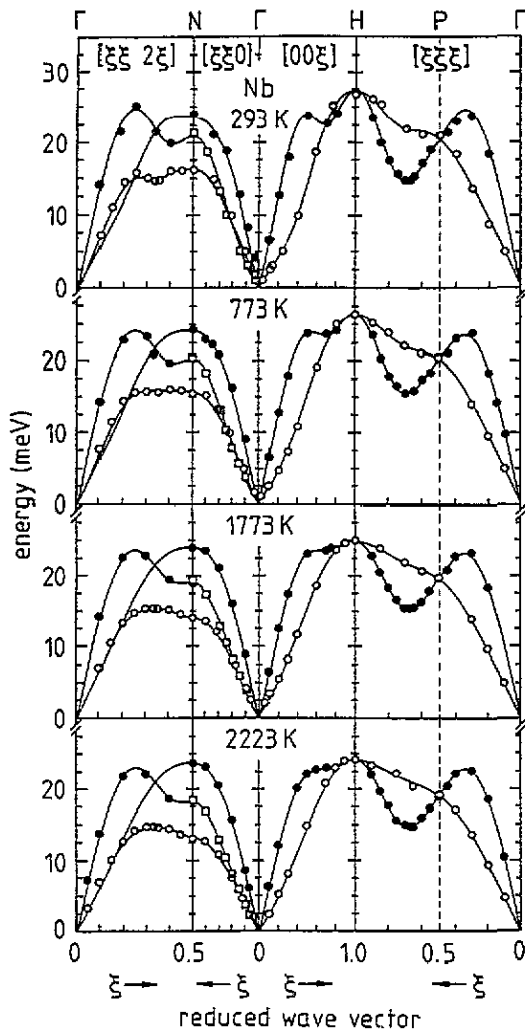
Figure 1. The phonon dispersion of Nb measured at different temperatures. The lines are fits by Born–von Kármán force constants up to the sixth-neighbour shell, table 2, and initial slopes are constrained according to the experimental elastic constants [19].

With higher temperatures these effects are smeared out. Keeping this in mind, we used the Born–von Kármán model as a parameterization, regardless of the underlying physical effects.

Table 1. Elastic constants of Nb at different temperatures after [19]. Values are in 10^{11} N m^{-2}.

T (K)	C_{11}	C_{12}	C_{44}	C'
293	2.438	1.325	0.276	0.556
773	2.330	1.257	0.302	0.536
1773	2.140	1.233	0.357	0.454
2223	2.027	1.228	0.374	0.400

The use of the Gilat and Raubenheimer method [22] allows then the computation of the phonon density of state $g(\omega)$—see figure 3—which in turn serves to calculate thermodynamic quantities [23]—see table 3. One finds in $g(\omega)$ three pronounced peaks, the lowest of which, around 15 meV, is of importance in the following discussion. It originates
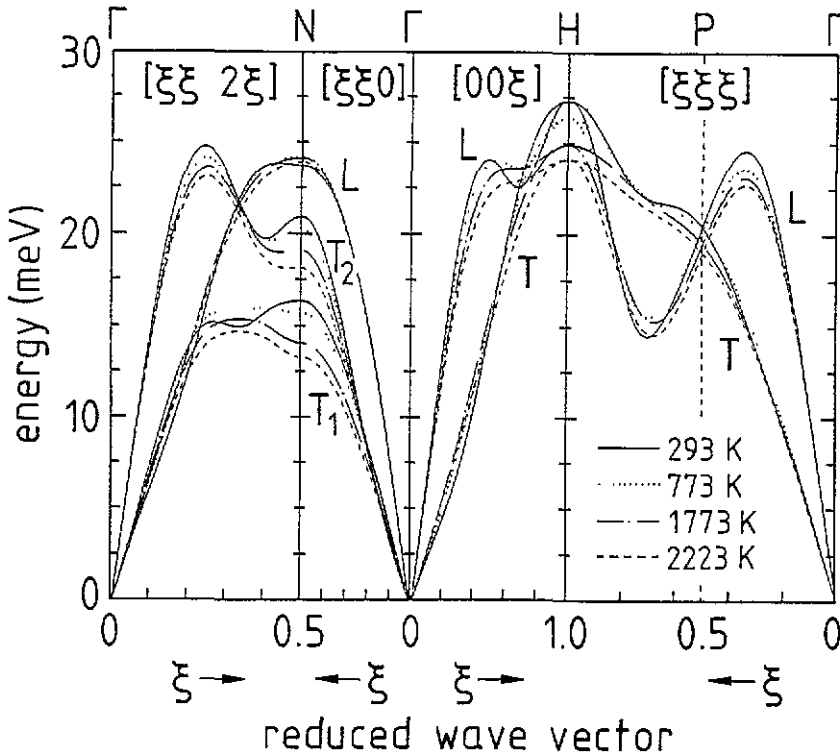
Figure 2. A comparison of the fitted phonon dispersion curves of Nb at different temperatures.

Table 2. Interatomic force constants Φ_{ij}^{m} in Nb in units of N m^{-1}, obtained from Born–von Kármán fits to the dispersions including six NN shells.

Φ_{ij}^{m}	$T = 293$ K	$T = 773$ K	$T = 1773$ K	$T = 2223$ K
1_{xx}	13.182	13.314	12.766	11.699
1_{xy}	9.951	9.691	10.029	10.068
2_{xx}	13.330	13.324	12.109	12.465
2_{yy}	−2.072	−2.164	−2.047	−1.882
3_{xr}	2.505	2.429	2.236	1.800
3_{zz}	−6.283	−5.032	−3.740	−3.424
3_{xy}	1.241	0.914	1.101	0.977
4_{xx}	4.200	2.713	1.571	1.344
4_{yy}	−0.413	−0.268	−0.281	−0.068
4_{yz}	−1.220	−0.429	−0.318	−0.209
4_{xy}	1.111	0.879	0.598	0.562
5_{xx}	−1.276	−0.879	−0.400	−0.550
5_{xy}	−1.168	−0.864	−0.556	−0.433
6_{xx}	−7.043	−4.542	−2.512	−1.766
6_{yy}	1.506	0.634	0.274	0.312

from the dispersionless part of the $T_1[\xi\xi2\xi]$ phonon branch, and contains all the phonons involved in the transformation of an open BCC structure to a close-packed structure [6]. This part of the dispersion stiffens from RT to 773 K, then reverses its temperature dependence and clearly falls below the RT value at 2223 K. As mentioned in section 1, the migration energy H^m can be estimated from the phonon dispersion [7]

$$H^{\mathrm{m}} = \alpha (G^0)^{-1} a^2 \qquad G^0 = \int \frac{g(\omega)}{M\omega^2}\, d\omega. \tag{1}$$

The basic idea of this model is that the migration enthalpy separates into a structural term αa^2, common to all BCC structures, and a term $(G^0)^{-1}$ reflecting the dynamical peculiarities of the element under consideration. $\alpha_{\mathrm{BCC}} = 0.0130(7)$ has been determined by computer simulation [7] and a is the lattice parameter. The element specific part of the displacement potential enters by the minus-second moment of $g(\omega)$, i.e. the static Green function G^0. It is due to this weighting with ω^{-2} that low-energy phonons are the essential quantity for the probing of the migration barrier. This model is similar to the earlier one of Flynn [24], who related H^{m} to the elastic constants, i.e. to the long-wavelength phonons. In contrast to that of Flynn, our model accounts for all phonons, in particular those at the Brillouin zone boundary. The latter are of importance because the short-wavelength phonons achieve the maximal displacement of neighbouring atoms relative to each other.
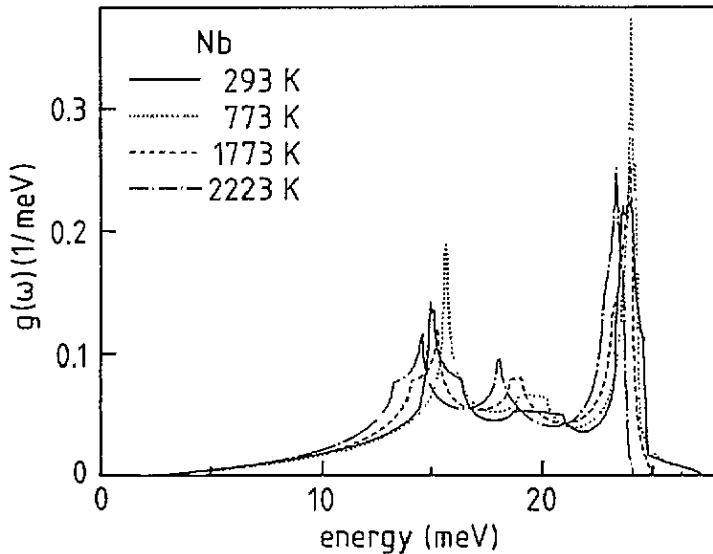

Figure 3. The phonon density of state $g(\omega)$ of Nb at different temperatures.

Table 3. Lattice parameter a, mean square displacement $\langle u_x^2 \rangle$, Debye temperature θ_{-2}, lattice entropy S_{vib}, migration enthalpy H^{m}, formation entropy S^{f}, and static lattice Green function G^0 for Nb. θ_{-2} is defined by $3\hbar/(k_{\mathrm{B}}\theta_{-2})^2 = \int_0^{\omega_{\mathrm{m}}} \omega^{-2} g(\omega)\, d\omega$.

T (K)	a (Å)	$\langle u_x^2 \rangle$ (Å^{-2})	Θ_{-2} (K)	$S_{\mathrm{vib}}(k_{\mathrm{B}}/\mathrm{atom})$	H^{m} (eV)	$S^{\mathrm{f}}(k_{\mathrm{B}}/\mathrm{atom})$	G^0(cm/dyn)
293	3.30	0.0062	274.7	4.21	0.59	2.12	-1.51×10^{-5}
296[a]	3.30	0.0063	274.0	4.26	0.58	—	-1.51×10^{-5}
700[a]	3.31	0.0145	275.2	6.77	0.60	—	-1.48×10^{-5}
773	3.31	0.0154	281.2	7.04	0.62	2.08	-1.44×10^{-5}
900[a]	3.32	0.0177	282.8	7.50	0.62	—	-1.44×10^{-5}
1773	3.34	0.0360	277.7	9.59	0.62	2.05	-1.47×10^{-5}
2223	3.36	0.0480	269.3	10.37	0.58	2.06	-1.57×10^{-5}

[a] From phonon measurements of Powell et al [13].

Because the lattice potentials are anharmonic, the phonon energies shift with temperature and H^m has to change with temperature, too. Table 3 and the inset in figure 5 show the variation of H^m with temperature†. Due to the dominance of the low-energy phonons, H^m first increases with temperature by more than 10% and decreases again at the higher temperatures where the diffusion constants are known. This inversion of the temperature dependence reflects the position of Nb in between the group IV and VI metals. In β-Ti, β-Zr, and β-Hf, H^m increases with temperature but it decreases in Cr [8] or Mo [9] where BCC is the only stable phase. Obviously the d electron density is the control parameter. Increasing the d electron density, with its characteristic bonding, entangles the motion of [111] NN chains [5] and stabilizes the BCC lattice. Phonons along $T_1[\xi\xi2\xi]$ harden with increasing e/a—figure 4—and hence so does H^m. The temperature variations of H^m for β-Zr and Cr are considerable (see figure 2(b) of [7]). According to its intermediate position, the variations in Nb are less pronounced.
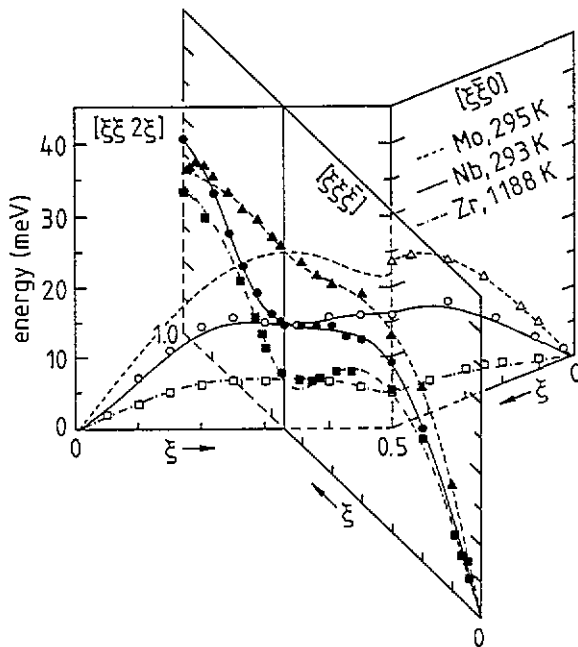

Figure 4. A comparison of phonon branches along $[\xi\xi\bar{\xi}]$, $[\xi\xi2\xi]$, and $[\xi\bar{\xi}0]$ propagation for β-Zr [6], Nb, and Mo [9].

The low values of H^m are in agreement with quenching experiments in Nb by Schwirtlich and Schultz [25], who find $H^m = 0.6$–0.9 eV depending on the different assumptions on the formation entropy S^f. They pointed out the low quenching-in resistivity in Nb, which indicates highly mobile vacancies. This is also supported by the low stage III annealing temperatures after electron irradiation detected by Faber *et al* [26] who find $H^m = 0.55$ eV. Calculating H^m according to Flynn [24], i.e. on the basis of elastic constants at 4 K, $H^m = 0.56$ eV. From high-temperature positron annihilation experiments Maier *et al* [27] deduce a vacancy formation enthalpy $H^f = 2.6(3)$ eV. Drittler [28] estimates by an *ab initio* generalized KKR–Green function method $H^f = 2.84$ eV at 0 K.

† A major uncertainty in determining the *absolute* value of H^m, according to (1), originates from the extrapolation between phonon branches in $g(\omega)$, because phonons have only been measured along symmetry directions. This systematic error is estimated to be less than 10% of H^m and certainly concerns much less the *relative* changes reported here (see the error bars in figure 5).

Using our average estimate $H^m \cong 0.6$ eV and $H^f \cong 2.6$–2.9 eV one obtains an activation energy $Q = 3.2$–3.5 eV. This value is in fair agreement with direct determinations of Q by means of radio tracer experiments, where in the temperature range from 1350 K to 1870 K $Q = 3.62$ eV [11] was found. However, at higher temperatures a slight upward curvature in the Arrhenius presentation of $D(T)$ is discernible and fitting all $D(T)$ over the whole range by a single exponential one finds $Q = 4.1$ eV, a value from which $H^f \simeq 3.5$ eV would follow when $H^m \cong 0.6$ eV is used.

According to the theory of Vineyard [29], the vacancy formation entropy S^f can be seen as the difference between the vibrational entropies of (i) the perfect lattice and (ii) a lattice with one vacancy and an additional atom on the surface, $S^f = S_{vib}(\text{perfect}) - S_{vib}(\text{def})$. Results for Nb are given in table 3; details of the calculation are reported elsewhere [7,30]. We find an almost temperature independent $S^f \cong 2.1$. This is higher than S^f in FCC or HCP metals but can be understood from the more open BCC structure and the covalent contributions to the bonding in transition metals.

Let us see now whether the calculated values of H^m and S^f for diffusion via NN vacancies are compatible with $D(T)$ [10–12]. In the usual *ansatz* for

$$D(T) = \nu_0 f a^2 \exp\{(S^m(T) + S^f(T))/k_B\} \exp\{-(H^m(T) + H^f(T))/k_B T\} \tag{2}$$

we have now introduced explicit temperature dependences for all thermodynamic quantities. ν_0 is the attempt frequency and $f = 0.727$ the correlation factor for self-diffusion via NN vacancies in the BCC structure. These latter two values are assumed to be temperature independent.

Values of $H^m(T)$ were determined by (1) for the temperatures where phonon measurements are available and are shown in the inset in figure 5. Because $H^m(T)$ first increases, then decreases with temperature, its temperature dependence is approximated by a quadratic polynomial $H^m(T) = H_0^m + H_1^m T + H_2^m T^2$. $H_0^m = 0.56$ eV, $H_1^m = 1.1 \times 10^{-4}$ eV K^{-1} and $H_2^m = -4.3 \times 10^{-8}$ eV K^{-2} are found. The corresponding curve is also shown in the inset in figure 5. Once the functional form of $H^m(T)$ is given, and assuming that H^f also changes with temperature, the thermodynamic relation

$$\partial H^{m/f}/\partial T = T \partial S^{m/f}/\partial T \tag{3}$$

defines the temperature dependence of $S^{m/f}$. The temperature dependent activation energy Q is given by

$$Q \equiv -\partial \ln\{D(T)\}/\partial(1/k_B T) = (H_0^m + H_0^f) + (H_1^m + H_1^f)T + (H_2^m + H_2^f)T^2 = H(T). \tag{4}$$

Using this relation and the polynomial description of the temperature dependent $H^m(T)$, two fits of $D(T)$ were performed:

(i) H^f, $S^f = $ constant and $S^m(T) = S_0^m + H_1^m \ln T + 2H_2^m T$;

(ii) $H^f(T) = H_0^f + H_1^f T + H_2^f T^2$, which according to (3) requires $S^{m/f} = S_0^{m/f} + H_1^{m/f} \ln T + 2H_2^{m/f} T$.

Fit (i) gives a temperature independent value $H^f = 3.5$ eV. According to (4) and with $H_{1/2}^f = 0$ a downward curvature of the Arrhenius plot of $D(T)$ is produced in the temperature range where diffusivities have been measured. Therefore fit (i) clearly fails to reproduce $D(T)$. Further, the prefactor $\nu_0 \exp\{(S^m + S^f)/k_B\} = 4.7 \times 10^5$ THz seems non-physical because it is too far from the Debye frequency.

Allowing both H^m and H^f to be temperature dependent—case (ii)—the upward curvature in the Arrhenius plot of $D(T)$ is reproduced reasonably well. In the temperature
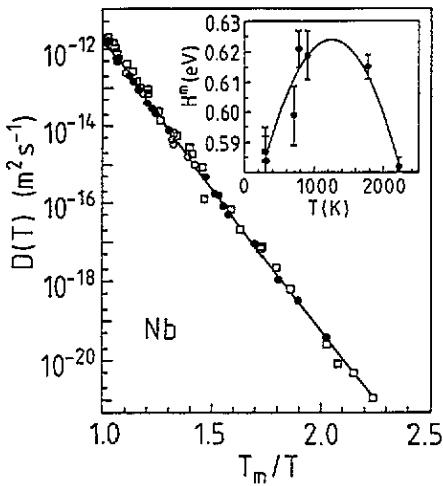
Figure 5. The self-diffusivity $D(T)$ in Nb. Data are from [10] (□), [11] (●) and [12] (○). The line is the fit for case (ii) (see the text). Inset: $H^m(T)$ as calculated by (1) (points) and a quadratic polynomial fit (full line) to all $H^m(T)$.

range where $H^m(T)$ has been determined values of $H^f(293 \to 2223 \text{ K}) = 3.0 \to 3.7$ eV are found, i.e. at higher temperatures $H^f(T)$ is definitely above the experimental and theoretical estimations discussed before. The prefactor $v_0 \exp\{(S_0^m + S_0^f)/k_B\} = 65$ THz fits very well to what one expects of NN vacancy diffusion. Using our calculated $S^f \cong 2.1k_B$/atom and assuming an attempt frequency $v_0 \cong 4$ THz, i.e. of the order of the first peak in the phonon density of state, a migration entropy $S^m \cong 0.7k_B$/atom is estimated.

5. Conclusion

Phonon frequencies in Nb measured at temperatures up to 2223 K shift with temperature, which indicates the importance of anharmonicity in BCC metals. Within the series of transition metals, this effect scales with the d electron density. Whereas in the β-phase of the group IV metals these phonons, which are related to the displacive phase transitions, stiffens with increasing temperature, the opposite happens in Group VI metals. According to its position in between these two extremes, Nb as a representative of group V metals shows much weaker temperature effects. Transverse phonons along $T_1[\xi\xi2\xi]$ first stiffen with increasing temperature and then decrease for $T \geqslant 1/2T_m$.

In the framework of the model of phonon controlled diffusion, the migration enthalpy H^m and the vacancy formation entropy S^f have been calculated. For NN vacancy jumps H^m depends on temperature; it increases up to $T \simeq 1/2T_m$ and decreases for higher temperatures. Excellent agreement is achieved with resistivity annealing. Also $S^f \cong 2.1k_B$/atom compares well with values of other BCC metals [7].

We have not calculated the vacancy formation enthalpy of H^f directly but, by means of our calculated $H^m(T)$ and $S^f(T)$, the tracer diffusivity $D(T)$ can be reproduced allowing H^f to be dependent on temperature, too. Because H^f is related to the electron density $n(\varepsilon)$ at the Brillouin zone (BZ) boundary [16] this requires a temperature dependent $n(\varepsilon)$. Characteristic changes of the phonon dispersion of Nb with increasing temperature—see section 3—are indicative that $n(\varepsilon)$ does indeed change with temperature. Restricting oneself to temperatures $T \leqslant 0.7T_m$ one derives a value of $H^f \leqslant 3.0$ eV, which is close to the theoretical estimate. For higher temperature $H^f(T)$ increases further and is definitely higher than $H^f = 2.6(3)$ eV as measured by positron annihilation.

One way to reconcile this contradiction is the introduction of a second diffusion mechanism, gaining in importance for $T > 1/2T_m$. However, it cannot be excluded that

the measured value of H^f is too low. First, the temperature dependence of the positron lifetime in Nb does not show any saturation [27] and highly mobile vacancies may truncate the result. Secondly, positron lifetime measurements in the β-phase of group IV metals do not at all show a vacancy caused increase of their lifetime [31], i.e. they indicate some fundamental problems of measuring vacancy concentrations in the high-temperature BCC metals by positron annihilation.

Acknowledgments

References

[1]   Peterson N L 1978 *Comment. Solid State Phys.* 8 93
[2]   Herzig C 1982 *Diffusion in Metals and Alloys, Dimenta-82* ed F J Kedves and D L Beke (Aedermannsdorf: Trans Tech) p 23
[3]   Petry W, Heiming A, Herzig C and Trampenau J 1991 *Defect Diffusion Forum* 75 211
      Köhler U and Herzig C 1988 *Phil. Mag.* A 58 769
[4]   Falter C, Ludwig W, Selmke M and Zierau W 1982 *Phys. Lett.* 90A 250
      Falter C, Ludwig W, Zierau W and Selmke M 1983 *Phys. Lett.* 93A 298
[5]   Ho K-M, Fu C-L and Harmon B N 1983 *Phys. Rev.* B 28 6687; 1984 *Phys. Rev.* B 29 1575
[6]   Petry W 1991 *Phase Transitions* 31 119
[7]   Schober H R, Petry W and Trampenau J 1992 *J. Phys.: Condens. Matter* 4 9321
[8]   Trampenau J, Petry W and Herzig C 1993 *Phys. Rev.* B 47 3132
[9]   Zarestky J, Stassis C, Harmon B N, Ho K-N and Fu C L 1983 *Phys. Rev.* B 28 697
[10] Lundy T S, Winslow F R, Pawel R E and McHargue C J 1965 *Trans. Met. Soc. AIME* 233 1533
[11] Einziger R E, Mundy J N and Hoff H A 1978 *Phys. Rev.* B 17 440
[12] Bussman W, Herzig C, Hoff H A and Mundy J N 1981 *Phys. Rev.* B 23 6216
[13] Powell B M, Woods A D B and Martel P 1972 *Neutron Inelastic Scattering* vol 43 (Vienna: IAEA)
[14] Sinha S K and Harmon B N 1976 *Superconductivity in d- and f-band Metals* vol 269 (New York: Plenum)
[15] Varma C M and Weber W 1979 *Phys. Rev.* B 19 6142
[16] Miedema A R 1979 *Z. Metallk.* 70 345
[17] Nakagawa Y and Woods A D B 1963 *Phys. Rev. Lett.* 11 271
[18] Powell B M, Martel P and Woods A D B 1977 *Can. J. Phys.* 55 1601
[19] Talmor Y, Walker E and Steinemann S 1977 *Solid State Commun.* 23 649
[20] Rebonato R and Broughton J Q 1987 *Phil. Mag. Lett.* 55 225
[21] Singh N, Banger N S and Singh S P 1989 *Phys. Rev.* B 39 12912
[22] Gilat G and Raubenheimer L J 1966 *Phys. Rev.* 144 390
[23] Hui J C K and Allen P B 1975 *J. Phys. C: Solid State Phys.* 8 2923
[24] Flynn C P 1968 *Phys. Rev.* 171 682
[25] Schwirtlich I A and Schultz H 1980 *Phil. Mag.* A 42 613
[26] Faber K, Scheikhardt J and Schultz H 1974 *Scr. Metall.* 8 713
      Faber K and Schultz H 1977 *Radiat. Eff.* 31 157
[27] Maier K, Peo M, Saile B, Schaefer H E and Seeger A 1979 *Phil. Mag.* A 40 701
[28] Drittler B H 1991 *Berichte des Forschungszentrums Jülich* 2445
[29] Vineyard G H 1957 *J. Phys. Chem. Solids* 3 121
[30] Hatcher R D, Zeller R and Dederichs P H 1979 *Phys. Rev.* B 19 5083
[31] Hood G M, Schultz R J and Carpenter G J C 1976 *Phys. Rev.* B 14 1503
      Hood G M and Schultz R J 1977 *J. Nucl. Mater.* 67 207